WWW.IJRPR.COM

International Journal of Research Publication and Reviews

Journal homepage: www.ijrpr.com ISSN 2582-7421

NUMERICAL INVESTIGATION OF FLOW-PROPERTY CHANGES ACROSS NORMAL SHOCK WAVES IN SUPERSONIC AIRFLOW

Muskaan Banu[1] , Bhavyashree M[2], Itika Sharma[3], Ayeesha MS[4], Anushree M[5], Khushwanth[6], S Kalyan Yadav[7]

Department of Aeronautical Engineering, MVJ College of Engineering, Bengaluru, India

ABSTRACT :

A normal shock wave is an irreversible compression phenomenon in which a supersonic stream is abruptly converted into a subsonic stream. The present report examines the changes in Mach number, static pressure, density, temperature, stagnation pressure and entropy for air represented as a calorically perfect gas with a constant specific-heat ratio of $\gamma = 1.4$. The governing relations are derived from conservation of mass, momentum and energy and are evaluated over an upstream Mach-number range extending from 1.2 to 3.5. The results show that stronger shocks produce larger increases in static pressure, density and temperature, while the downstream Mach number and stagnation-pressure recovery decrease. A detailed literature survey is included to place the one-dimensional normal-shock model in the wider context of classical gas dynamics, experimental shock studies, shock-wave/boundary-layer interaction, computational methods and aerospace applications. The ideal-gas calculation is intended as a transparent baseline for preliminary analysis and for comparison with more complex numerical or experimental work.

Keywords Normal shock; compressible flow; supersonic aerodynamics; Mach number; stagnation pressure; entropy generation; shock-boundary-layer interaction.

1. INTRODUCTION

The study of compressible fluid flow is an important branch of aerodynamics and gas dynamics, particularly in the design and analysis of aircraft, propulsion systems, high-speed vehicles, wind tunnels, and aerospace testing facilities. Unlike incompressible flow, in which density changes are often small enough to be neglected, compressible flow involves significant variations in density, pressure, and temperature due to changes in flow velocity and thermodynamic conditions. These variations become particularly important when the flow velocity approaches or exceeds the local speed of sound. In such conditions, the relationship between pressure disturbances and fluid motion changes significantly, resulting in several important flow phenomena, including shock waves, expansion waves, choking, and compressibility effects. Among these phenomena, shock waves are especially important because they produce rapid changes in the thermodynamic and aerodynamic properties of a moving gas.

A shock wave is a thin region in a compressible flow across which the pressure, density, temperature, velocity, and other flow properties change rapidly. It commonly develops when a supersonic flow undergoes compression or encounters a change in geometry or operating conditions that requires the flow to adjust. In supersonic flow, disturbances cannot travel upstream through the undisturbed gas because the flow velocity exceeds the local speed of sound. Consequently, compression disturbances may accumulate into a shock wave, producing an abrupt transition between two flow states. Shock waves are characterized by strong gradients in flow properties and by irreversible thermodynamic changes. Their presence can significantly influence aerodynamic performance, pressure recovery, energy conversion, thermal loading, and the overall efficiency of high-speed flow systems.

Shock waves can be classified according to their orientation relative to the incoming flow and the physical configuration in which they occur. The principal types include normal shock waves, oblique shock waves, and detached bow shock waves. A normal shock wave is oriented perpendicular to the incoming flow direction, whereas an oblique shock wave is inclined to the upstream velocity. A detached bow shock forms ahead of a blunt body moving through a supersonic stream. Although these configurations occur in different aerodynamic situations, they are connected through the conservation principles governing compressible flow. The normal shock is particularly useful as a fundamental model because its geometry allows the changes in flow properties to be examined using one-dimensional conservation equations. It therefore provides a convenient starting point for understanding more complicated shock systems encountered in practical aerospace applications [1]–[3].

A normal shock wave occurs when a supersonic stream passes through a stationary shock surface perpendicular to the direction of flow. Before

crossing the shock, the gas has a supersonic Mach number, while immediately after crossing it, the flow becomes subsonic. This transition is accompanied by an increase in static pressure, density, and static temperature, together with a decrease in flow velocity. The upstream and downstream states are connected by the conservation of mass, momentum, and total energy. For a stationary, adiabatic shock without shaft work, these conservation laws establish the fundamental relationships between the properties before and after the shock. When air is represented as a calorically perfect gas with a constant ratio of specific heats, these relationships can be expressed as algebraic equations involving the upstream Mach number and the specific-heat ratio [1], [3].

The Mach number is one of the most important parameters in normal-shock analysis. It is defined as the ratio of the local flow velocity to the local speed of sound. The upstream Mach number determines the strength of the shock and strongly influences the changes in pressure, density, temperature, velocity, and stagnation pressure. When the upstream Mach number is only slightly greater than unity, the shock is relatively weak and the changes in the flow properties are comparatively small. As the upstream Mach number increases, the shock becomes stronger, producing a greater static-pressure rise, a larger temperature increase, and more substantial flow deceleration. At the same time, the downstream Mach number decreases, although the density ratio approaches a finite limiting value in the ideal-gas model. Understanding these trends is essential for interpreting the performance of supersonic inlets, diffusers, nozzles, and other compressible-flow components [1], [2].

The thermodynamic behaviour of a normal shock is also important because the process is irreversible. Although the static pressure and temperature increase across the shock, the stagnation pressure decreases. Stagnation pressure represents the pressure that would be obtained if the moving gas were brought to rest isentropically. In an ideal reversible process, stagnation pressure remains constant. However, a normal shock generates entropy, which results in a loss of stagnation pressure. This loss represents an important performance penalty in aerospace propulsion systems because it reduces the total pressure available to downstream components. For example, in a supersonic aircraft inlet, the incoming air must be compressed and decelerated before entering the compressor. A normal shock can achieve the required transition from supersonic to subsonic flow, but the associated stagnation-pressure loss can reduce engine performance. Therefore, an assessment of normal-shock behaviour must consider not only the static-pressure rise but also the irreversible losses associated with the process [1]–[3].

The conservation of energy provides further insight into the changes occurring across a normal shock. For an adiabatic shock without shaft work, the total enthalpy remains constant. As the gas passes through the shock, its velocity decreases and part of its organized kinetic energy is converted into internal energy. Consequently, the static temperature increases. For a calorically perfect gas, the stagnation temperature remains constant because the total enthalpy is conserved, and the specific heat is assumed constant. This distinction between static and stagnation properties is essential in compressible-flow analysis. Static properties describe the local thermodynamic state of the moving gas, whereas stagnation properties describe the state associated with bringing the gas to rest under the appropriate idealized conditions. Confusing these quantities can lead to incorrect interpretations of shock behaviour and inaccurate engineering calculations.

Normal-shock theory has been established through classical studies of gas dynamics and is documented in standard engineering references. NACA Report 1135, Equations, Tables, and Charts for Compressible Flow, provides a widely used collection of compressible-flow equations, including normal- and oblique-shock relations [1]. NASA Glenn Research Center also presents the governing normal-shock equations and their physical interpretation in an educational format suitable for preliminary engineering calculations [2]. These references demonstrate that the ideal normal shock is a well-established theoretical problem. Its importance lies not only in the ability to calculate property changes but also in its usefulness as a reference case for checking experimental observations and computational fluid dynamics simulations.

Despite the usefulness of the ideal normal-shock model, actual shock waves may exhibit more complicated behaviour than the one-dimensional theory predicts. In real aerodynamic systems, shock waves can interact with boundary layers, turbulent flow structures, walls, and other shocks. These interactions can lead to boundary-layer separation, fluctuating pressure distributions, local heating, changes in skin friction, and unsteady shock motion. Experimental studies and numerical investigations have shown that shock-wave/boundary-layer interactions can be difficult to predict accurately because their behaviour depends on Mach number, Reynolds number, boundary-layer thickness, turbulence characteristics, geometry, and downstream conditions [5]–[13]. Such effects are especially important in supersonic aircraft inlets and internal ducts, where excessive flow separation and total-pressure loss may affect operating stability and propulsion efficiency.

Computational fluid dynamics has become an important method for studying compressible flows containing shock waves. Numerical methods can be used to calculate the flow field, visualize shock locations, determine pressure and temperature distributions, and examine the influence of geometry and boundary conditions. However, a numerical solution must be checked against appropriate theoretical or experimental reference data. The analytical normal-shock relations provide a useful verification case because the upstream and downstream states can be calculated directly from conservation laws. By comparing numerical predictions with theoretical values for downstream Mach number, pressure ratio, density ratio, temperature ratio, and stagnation-pressure recovery, the consistency of a computational model can be assessed. Nevertheless, agreement with ideal normal-shock relations does not automatically establish that a model accurately predicts more complex phenomena such as turbulent separation, wall heat transfer, or three-dimensional shock interactions [27]–[45].

Another important consideration is the range of validity of the perfect-gas assumption. In the present investigation, air is treated as a calorically perfect gas with a constant specific-heat ratio of □\gamma = 1.4□. This assumption simplifies the governing equations and allows the influence of upstream Mach number to be examined systematically. It is appropriate for establishing a basic theoretical understanding of normal-shock behaviour and for performing many preliminary engineering calculations. However, at sufficiently high temperatures, the specific heats of air vary with temperature, and

molecular vibrational excitation, dissociation, or ionization may become important. Under such conditions, a more detailed thermodynamic model is required to predict the post-shock state accurately. The perfect-gas formulation should therefore be understood as a clearly defined engineering approximation rather than a universal description of every high-speed flow condition [14], [25], [26].

The present study focuses on the systematic evaluation of normal-shock properties for upstream Mach numbers ranging from 1.2 to 3.5. This range provides an opportunity to examine the gradual transition from relatively weak to substantially stronger normal shocks within a consistent theoretical framework. The analysis calculates the downstream Mach number, static-pressure ratio, density ratio, static-temperature ratio, velocity ratio, stagnation-temperature ratio, stagnation-pressure recovery, and entropy change. The results are interpreted to establish how increasing upstream Mach number influences compression, deceleration, temperature rise, and irreversible pressure loss. Standard sea-level reference conditions are also used to illustrate how dimensionless property ratios can be related to representative dimensional values of pressure, temperature, density, and velocity.

The central motivation of this investigation is to connect the fundamental equations of compressible-flow theory with their physical meaning and engineering significance. Rather than treating the normal-shock equations as isolated mathematical expressions, the study examines how each calculated property reflects the conservation of mass, momentum, and energy and the second law of thermodynamics. The results are used to identify the trends that govern normal-shock behaviour and to explain why stronger shocks produce more substantial changes in static properties and greater losses in stagnation pressure. The analysis also establishes a theoretical baseline that can be used for comparison with more advanced computational or experimental studies.

In addition, this investigation recognizes the distinction between a theoretical model and a complete prediction of a practical aerospace system. The one-dimensional normal-shock relations determine the net change between uniform upstream and downstream states, but they do not resolve the internal viscous structure of the shock or represent the full effects of turbulence, wall interactions, three-dimensional geometry, or high-temperature chemistry. These limitations are important when extending the results to actual aircraft inlets, propulsion systems, shock tubes, nozzles, and high-speed vehicles. By clearly identifying the assumptions and limitations of the model, the study provides a sound basis for interpreting the results and for identifying possible extensions to more advanced gas-dynamic analysis.

Overall, the investigation presents a structured analytical and numerical study of normal shock waves in supersonic air. It combines established theoretical relations with calculated property ratios, graphical interpretation, and a review of relevant research. The findings are intended to strengthen the understanding of shock-wave physics and demonstrate the relationship between Mach number, compression, energy conversion, entropy generation, and stagnation-pressure loss. By establishing a reproducible reference solution for a selected range of upstream Mach numbers, the study provides a foundation for future work involving oblique shocks, shock-wave/boundary-layer interactions, computational fluid dynamics, and more realistic thermodynamic models for high-speed aerospace applications.

2. LITERATURE SURVEY

The literature survey is organized as a paper-style critical review. Each subsection is numbered consecutively (2.1–2.27), moving from classical normal-shock theory and experimental evidence to shock interactions, numerical methods, real-gas effects and engineering applications. The discussion distinguishes established analytical results from findings that depend on viscous, turbulent, unsteady or high-temperature physics. References are cited by number and collected in one bibliography at the end.

2.1 Scope and organization of shock-wave literature [1–3, 19–25]

Research on shock waves spans classical gas dynamics, experimental aerodynamics, propulsion, high-enthalpy flow and computational fluid dynamics. Within this broad field, a normal shock is a useful reference problem because its geometry is simple and its upstream and downstream states can be connected through conservation laws. The literature can be organized into several overlapping themes: derivation of jump relations; tabulation and engineering use of perfect-gas solutions; measurements in shock tubes and wind tunnels; interaction with boundary layers and turbulence; real-gas and high-temperature effects; and the use of analytical solutions to verify numerical methods. This chapter follows that progression rather than treating each publication as an isolated item.

The central distinction throughout the literature is between the ideal discontinuity model and the finite-thickness physical shock. The jump model predicts the net changes between uniform states on either side. Viscosity and heat conduction, however, are responsible for the internal structure and entropy production within the thin shock layer. For preliminary engineering calculations, the jump relations are often sufficient. For wall heat transfer, separation, unsteadiness or detailed internal profiles, additional physical modelling and experimental evidence are needed. This distinction provides the framework for interpreting the present calculation.

Relevance to this project: this topic establishes why a one-dimensional normal-shock calculation is a useful starting point, while also defining what it cannot predict.

2.2 Early foundations of compressible gas dynamics [19–23]

The theoretical foundation of normal-shock analysis is the conservation of mass, momentum and total energy applied to a control volume moving with, or fixed to, the shock. The resulting jump conditions are independent of the detailed shape of the velocity and temperature profiles inside the shock,

provided the states sufficiently far upstream and downstream are uniform. For a calorically perfect gas, the equation of state and constant specific heats close the system and yield explicit relations between upstream Mach number and downstream properties. This formulation makes the normal shock one of the standard canonical problems in compressible-flow theory.

Classical gas-dynamics treatments emphasize that a shock is not an isentropic compression. Static pressure and temperature increase, but entropy also increases and stagnation pressure decreases. Total temperature remains constant for an adiabatic shock without shaft work because total enthalpy is conserved. These statements are important because they distinguish the shock from a reversible diffuser or an isentropic compression process. The modern engineering interpretation remains rooted in this classical conservation-law framework, which is also the basis of the equations used in the present report [1], [3].

Critical observation: the analytical relations are strongest when the assumptions are stated explicitly and the upstream and downstream states are clearly defined.

2.3 The contribution of NACA Report 1135 [1, 2]

Ames Research Staff's NACA Report 1135, Equations, Tables, and Charts for Compressible Flow, is a major engineering reference for perfect-gas compressible-flow calculations. Its treatment includes normal and oblique shock waves and presents the basic jump equations together with tabulated and graphical information. The report explicitly notes that isentropic relations apply on either side of a shock but not across the discontinuity; the shock jump itself must satisfy mass, momentum and energy conservation. This separation between smooth-flow relations and shock jump conditions is fundamental to practical calculation [1].

The value of NACA 1135 is not limited to the normal-shock formulas. It collects a consistent set of compressible-flow relations that allow the shock solution to be connected to upstream and downstream isentropic regions. Such combinations are required in inlet and nozzle analysis, where a shock may be embedded within a larger flow system. In the present study, the normal-shock ratios are used as standalone property-change measures, but the historical report provides the broader framework for integrating those ratios into a complete aerodynamic component calculation.

Implication: the present report uses this research as a theoretical baseline and does not claim to reproduce all the phenomena discussed in the wider literature.

2.4 Conservation of mass and momentum across a shock [1, 3, 19–23]

The continuity relation requires the mass flux to remain constant across a stationary shock: density multiplied by velocity is the same on both sides. Since density rises through a normal shock, the downstream velocity must decrease. The momentum equation balances static pressure and momentum flux. The rise in static pressure is therefore associated with the reduction in the streamwise momentum flux. These relations explain why the shock produces a compressed, slower downstream state rather than simply changing pressure independently of the velocity and density fields.

In the perfect-gas normal-shock solution, the density ratio is bounded for a fixed ratio of specific heats, whereas the pressure ratio continues to increase with upstream Mach number. This difference matters when interpreting high-Mach-number results: a very large pressure rise does not imply an equally unbounded density increase. The continuity and momentum equations also provide useful numerical checks. If the calculated downstream velocity, density and pressure do not satisfy the corresponding flux balances, the implementation or the use of units and property definitions should be reviewed.

Relevance to this project: this topic establishes why a one-dimensional normal-shock calculation is a useful starting point, while also defining what it cannot predict.

2.5 Energy conservation and stagnation properties [1–3, 20–23]

For an adiabatic shock with no shaft work, the steady-flow energy equation requires the sum of static enthalpy and kinetic energy to remain constant. As the flow decelerates, part of its organized kinetic energy is converted into internal energy, producing a higher static temperature. For a calorically perfect gas, enthalpy is proportional to temperature, so the energy equation can be written directly in terms of the static-temperature rise and the velocity reduction. This is the thermodynamic basis for the temperature increase observed across a normal shock.

The stagnation temperature is unchanged in this ideal adiabatic model because it is proportional to total enthalpy for a fixed gas model. Stagnation pressure behaves differently: it decreases because the process is irreversible. The literature consistently treats total-pressure recovery as a key measure of shock loss in propulsion and inlet design. A report that discusses only static-pressure rise therefore gives an incomplete account of shock performance. The present investigation includes both static-property ratios and stagnation-pressure recovery for this reason [1], [2].

Critical observation: the analytical relations are strongest when the assumptions are stated explicitly and the upstream and downstream states are clearly defined.

2.6 Entropy generation and irreversibility [1–3, 19–23]

The second law determines the physically admissible direction of a shock process. For a supersonic upstream state and subsonic downstream state, the entropy change is positive. In a calorically perfect gas, entropy change can be evaluated from the temperature and pressure ratios. The result approaches zero as the upstream Mach number approaches unity, because the shock becomes vanishingly weak. As shock strength increases, entropy generation grows and the associated stagnation-pressure loss becomes more severe.

The entropy viewpoint also clarifies why a normal shock cannot be treated as an ordinary isentropic compression. A reversible compression can increase static pressure while conserving stagnation pressure, whereas a shock creates entropy and reduces the pressure available for subsequent processes. In an inlet, this loss affects the pressure delivered to the compressor or combustor. In a nozzle, it can reduce the useful expansion

downstream. Thus, entropy generation is not merely a theoretical quantity; it is linked directly to component performance and propulsion-system efficiency.

Implication: the present report uses this research as a theoretical baseline and does not claim to reproduce all the phenomena discussed in the wider literature.

2.7 NASA Glenn educational formulation [2]

NASA Glenn Research Center's normal-shock educational material presents the standard relations for the downstream Mach number and static-property ratios. Its value is pedagogical: the equations connect the upstream Mach number and gas specific-heat ratio to the state immediately behind the shock. The material also places normal shocks within the wider topic of compressible flow and provides a clear engineering interpretation of the property changes. The NASA treatment is consistent with the conservation-law framework compiled in NACA Report 1135 [2].

For a study such as the present one, NASA's formulation provides an accessible independent reference for checking equation structure and physical trends. It is important, however, to distinguish educational explanatory material from a complete model of a real inlet. The algebraic relations describe a one-dimensional perfect-gas jump. They do not, by themselves, predict boundary-layer separation, shock motion, heat transfer to walls or three-dimensional distortion. Those issues are addressed in separate experimental and computational research streams.

Relevance to this project: this topic establishes why a one-dimensional normal-shock calculation is a useful starting point, while also defining what it cannot predict.

2.8 Normal shocks in shock tubes [4, 20, 21]

Shock tubes provide a controlled experimental environment for generating shock waves and studying rapid compression. A diaphragm separates regions of gas at different pressures; when it ruptures, a shock travels into the lower-pressure driven gas while an expansion wave propagates in the opposite direction. In the frame moving with the shock, the gas states on either side can be related using shock jump conditions. The normal-shock solution is therefore a central building block in the analysis of shock-tube experiments, even though the complete apparatus also requires unsteady-wave relations.

Davies and Edwards' experimental investigation of reflected-shock pressure-time profiles considered several gases and compared measurements with existing theories [4]. Their work illustrates that shock-tube records are affected by more than the initial ideal jump: reflected shocks, boundary-layer growth and the evolution of the test gas can influence measured pressure histories. This distinction is useful when comparing a steady normal-shock calculation with an experiment. The jump relation predicts an ideal state change; the experiment may include time-dependent and facility-specific effects.

Critical observation: the analytical relations are strongest when the assumptions are stated explicitly and the upstream and downstream states are clearly defined.

2.9 Experimental study of normal-shock and boundary-layer effects [5, 6]

Donaldson's 1944 work addressed the effects of interaction between a normal shock and a boundary layer, motivated by experimental observations that could not be explained by normal-shock theory alone [5]. The central implication is that the ideal one-dimensional shock model does not capture the full flow when a wall boundary layer is present. The boundary layer introduces a region of low-momentum fluid near the wall, and the imposed pressure rise can alter its development. Under sufficiently strong interaction, the boundary layer may separate and the shock structure may become more complex.

This historical result remains relevant to internal aerodynamics. In an actual duct or inlet, the shock is not isolated from the wall; it interacts with viscous layers that have developed upstream. Consequently, measured wall pressure, separation length and downstream velocity profiles may differ from values inferred from a uniform-flow normal-shock calculation. The ideal solution remains valuable as a baseline for the outer inviscid flow, but it must not be interpreted as a complete prediction of wall-bounded flow behaviour.

Implication: the present report uses this research as a theoretical baseline and does not claim to reproduce all the phenomena discussed in the wider literature.

2.10 Shock-wave and turbulent-boundary-layer interaction [6, 9, 45]

The interaction between a shock and a turbulent boundary layer became a major research topic because it influences inlet performance, aerodynamic loads, heat transfer and flow stability. Green's review of shock-wave/turbulent-boundary-layer interactions surveyed transonic through high-supersonic conditions and discussed the ability of contemporary methods to predict interaction structure [6]. The review highlighted the range of flow configurations and the difficulty of predicting separation and reattachment with a single simplified method.

A normal shock interacting with a turbulent boundary layer is not equivalent to the one-dimensional normal shock considered in the present calculations. The shock imposes an adverse pressure gradient on the boundary layer, and the resulting response depends on Mach number, Reynolds number, boundary-layer thickness and turbulence state. The interaction may include separation, a separated shear layer and a downstream recovery region. The literature therefore treats the normal-shock jump and the shock-boundary-layer interaction as related but distinct modelling problems.

Relevance to this project: this topic establishes why a one-dimensional normal-shock calculation is a useful starting point, while also defining what it cannot predict.

2.11 Experimental and numerical comparison at transonic speeds [7, 45]

Mateer, Brosh and Viegas reported experimental and computational results for a normal shock interacting with a turbulent boundary layer at a free-stream Mach number of 1.5 [7]. Their measurements included mean and fluctuating flow quantities, surface pressure, skin friction and separation length. The study identified a separated zone near the shock foot and compared the experimental flow with Navier–Stokes calculations using turbulence models. The computations reproduced qualitative features but did not fully match the measured separation extent and downstream skin friction.

This work demonstrates both the value and the limits of computational fluid dynamics. A model may capture the broad structure of the interaction while retaining quantitative errors in separation and wall-shear predictions. It also illustrates why validation requires more than comparing a single pressure ratio. A credible assessment may need surface pressure distributions, skin friction, velocity profiles, fluctuation levels and separation length. The present report does not attempt that level of modelling; it uses the ideal jump equations as a reproducible reference case.

Critical observation: the analytical relations are strongest when the assumptions are stated explicitly and the upstream and downstream states are clearly defined.

2.12 Shock-wave and turbulence interactions [8, 10]

Andreopoulos, Agui and Briassulis reviewed interactions between shock waves and several forms of turbulence, including homogeneous turbulence, shear flows, jets, wakes and boundary layers [8]. Their review describes the interaction as mutual: the shock can be deformed and made unsteady by turbulence, while the turbulence itself is modified by the passage through the shock. The response depends on shock strength and orientation, flow geometry, boundary conditions and the state of the incoming turbulence.

This research broadens the interpretation of shock strength. In a one-dimensional calculation, upstream Mach number is the principal variable controlling the jump. In turbulent flows, the incoming velocity fluctuations and length scales also influence the downstream field. The mean thermodynamic jump remains an important reference, but it does not fully describe the instantaneous flow. This is especially relevant to high-speed propulsion systems, where turbulence, shocks and wall effects coexist and may influence performance and structural loading.

Implication: the present report uses this research as a theoretical baseline and does not claim to reproduce all the phenomena discussed in the wider literature.

2.13 AGARD review of shock-boundary-layer interaction [9, 45]

Delery, Marvin and Reshotko's AGARDograph 280 provided a comprehensive review of shock-wave/boundary-layer interactions, including physical descriptions, experimental evidence, correlations and theoretical and numerical prediction methods [9]. The review discussed global methods, integral and finite-difference approaches, coupled flow-field methods, analytical multi-deck techniques and Reynolds-averaged Navier–Stokes methods. This breadth reflects the fact that interaction prediction is not reducible to a single closed-form equation.

The review is especially useful for distinguishing modelling levels. Integral methods can provide efficient estimates for selected boundary-layer quantities, while full-field numerical methods attempt to represent the coupled shock and viscous flow. Analytical approaches can reveal scaling behaviour and underlying mechanisms. Each method has limitations and requires validation against experiments. The normal-shock equations used in this report occupy the simplest end of this hierarchy and are most appropriate when the aim is to estimate ideal upstream-to-downstream property changes.

Relevance to this project: this topic establishes why a one-dimensional normal-shock calculation is a useful starting point, while also defining what it cannot predict.

2.14 Unsteadiness in shock interactions [10–12, 45]

Shock-boundary-layer interactions may be unsteady even when the mean operating condition is nominally steady. The shock can oscillate in response to large-scale structures in the incoming turbulent boundary layer, separation-bubble dynamics and coupling with downstream conditions. These motions influence time-averaged pressure distributions and can generate fluctuating aerodynamic loads. Research reviews emphasize that low-frequency motion may be important even when it is slower than the characteristic turbulent fluctuations in the incoming boundary layer [10], [11].

An algebraic normal-shock calculation cannot predict the amplitude or frequency of shock motion. It gives the mean ideal jump for a specified upstream state. Experimental diagnostics and time-resolved computational methods are needed to investigate unsteadiness. Nevertheless, the normal-shock relation remains useful for estimating the thermodynamic state associated with an instantaneous or representative shock strength. The distinction between mean jump properties and time-dependent interaction dynamics should be maintained when interpreting high-speed flow measurements.

Critical observation: the analytical relations are strongest when the assumptions are stated explicitly and the upstream and downstream states are clearly defined.

2.15 Heat transfer and thermal consequences [10, 11]

The temperature rise across a normal shock is associated with conversion of kinetic energy into internal energy. In practical components, this can influence thermal loading, material selection and cooling requirements. However, the static-temperature ratio predicted by the perfect-gas jump relation is not itself a wall heat-transfer prediction. Wall heat flux depends on the boundary layer, wall temperature, thermal conductivity, turbulence, flow residence time and the local shock-interaction structure.

Ligrani and co-authors' survey of shock-wave effects and interactions includes research on thermal transport and convective heat transfer in addition to

shock-boundary-layer physics and unsteadiness [10]. This is important because thermal effects can be coupled to the flow field. For example, a shock-induced change in boundary-layer state can modify heat transfer, while wall heating can in turn influence the boundary layer. The present one-dimensional model reports the ideal static-temperature rise but leaves these coupled thermal processes outside its scope.
Implication: the present report uses this research as a theoretical baseline and does not claim to reproduce all the phenomena discussed in the wider literature.

2.16 Three-dimensional shock-boundary-layer interactions [11, 12]

Many practical shock-boundary-layer interactions are three-dimensional. Aircraft intakes, swept surfaces, fins, struts and complex internal ducts produce shock systems whose orientation varies across the span and whose interaction with the boundary layer is spatially nonuniform. Sabnis and Babinsky reviewed three-dimensional shock-wave/boundary-layer interactions and discussed canonical configurations used to understand their flow physics [12]. Their review notes that practical intake flows are often three-dimensional and that the geometry can produce a wider range of interaction patterns than a two-dimensional model.
A three-dimensional interaction may include crossflow, streamwise vortices, skewed separation structures and nonuniform wall-pressure distributions. These features cannot be represented by a single normal-shock ratio. Yet the one-dimensional theory remains a useful local reference: the component of velocity normal to a shock is central to the jump, while tangential velocity is treated differently in oblique-shock analysis. This provides a conceptual bridge from the normal-shock model to more complex three-dimensional configurations.
Relevance to this project: this topic establishes why a one-dimensional normal-shock calculation is a useful starting point, while also defining what it cannot predict.

2.17 Recent review of three-dimensional interaction dynamics [11, 12]

Gaitonde and Adler's review of three-dimensional shock-wave/boundary-layer interaction dynamics summarizes progress in understanding separated interactions and highlights differences between two- and three-dimensional flow structures [11]. The review discusses the importance of configuration, shock orientation and the incoming boundary layer, and identifies areas where further study is required. The central message is that three-dimensional interactions cannot always be inferred by simply extending a two-dimensional picture across the span.
For engineering analysis, this means that a normal-shock baseline should be used with care. A practical inlet may experience a spatially varying shock strength, boundary-layer distortion and separation patterns that depend on the full geometry. Three-dimensional measurements and simulations are required when those details affect operability or performance. The present report deliberately isolates the normal component of the problem so that the basic thermodynamic changes can be examined without the additional complexity of full three-dimensional flow.
Critical observation: the analytical relations are strongest when the assumptions are stated explicitly and the upstream and downstream states are clearly defined.

2.18 Control of shock-boundary-layer interactions [12, 13, 45]

Researchers have investigated several strategies for controlling the adverse effects of shock-boundary-layer interactions. These include geometric shaping, boundary-layer bleed, passive devices, surface treatments and active flow-control methods. Jana and Kaushik's survey categorizes control techniques and evaluates the different approaches reported in the literature [13]. The review emphasizes that a technique effective for one shock arrangement or Mach-number range may not be universally effective.
Control is motivated by the penalties associated with separation, total-pressure loss, unsteadiness and heat transfer. In an inlet, the objective is often to maintain stable compression and avoid excessive distortion at the engine face. The normal-shock equations help quantify the ideal pressure recovery penalty for a given shock strength, but they do not select a control device or predict its effectiveness. That requires component-specific experiments or validated numerical modelling. The literature therefore places fundamental shock theory alongside system-level design and control research.
Implication: the present report uses this research as a theoretical baseline and does not claim to reproduce all the phenomena discussed in the wider literature.

2.19 Computational fluid dynamics and shock capturing [27–44]

Computational fluid dynamics has become an important tool for analysing compressible flows containing shocks. Numerical schemes must represent steep gradients without producing nonphysical oscillations, while also maintaining conservation and appropriate shock speed. Shock-capturing methods typically spread the discontinuity over several computational cells, so the computed internal shock thickness is numerical rather than a direct prediction of the physical thickness unless the governing physics and resolution are specifically designed for that purpose.
The ideal normal-shock solution is a valuable verification case for a compressible-flow solver. A one-dimensional calculation can be initialized with a supersonic upstream state and compared with the analytical downstream state. Useful checks include mass flux, momentum flux, total enthalpy, downstream Mach number and entropy increase. Agreement in these quantities helps establish that the numerical method handles a canonical discontinuity correctly. More complex validation is then needed for turbulence, boundary layers, heat transfer and three-dimensional geometries.
Relevance to this project: this topic establishes why a one-dimensional normal-shock calculation is a useful starting point, while also defining what it cannot predict.

2.20 Verification versus validation [27–44]

Verification asks whether a numerical calculation solves the chosen mathematical model correctly; validation asks whether that model adequately represents the physical system of interest. The normal-shock equations provide an analytical reference for verification because the ideal jump can be computed directly. A CFD result can be compared with the analytical ratios for pressure, density, temperature and Mach number. Differences may arise from numerical resolution, boundary conditions, flux formulation or inconsistent thermodynamic properties.

Validation requires experimental evidence that is relevant to the intended application. A calculation may agree closely with the ideal normal-shock solution and still fail to predict a real inlet if viscous interactions, heat transfer or three-dimensional effects are important. This distinction is consistent with the experimental literature on shock-boundary-layer interactions, where numerical methods have sometimes captured qualitative trends but missed quantitative features such as separation extent [7], [9]. The present work is an analytical-numerical baseline rather than an experimental validation study.

Critical observation: the analytical relations are strongest when the assumptions are stated explicitly and the upstream and downstream states are clearly defined.

2.21 Perfect-gas assumptions and their range of use [1, 3, 14, 19–26]

The perfect-gas normal-shock equations are based on an equation of state with constant specific heats and a fixed ratio of specific heats. For air under moderate-temperature conditions, $\gamma = 1.4$ is a common engineering approximation. This assumption gives compact algebraic expressions and makes it possible to compare different upstream Mach numbers without separately modelling molecular energy modes. It is particularly suitable for introductory analysis and many preliminary calculations.

At sufficiently high post-shock temperatures, the constant-specific-heat approximation becomes less accurate. Molecular vibrational excitation changes the effective heat capacity; at still higher enthalpy, dissociation and ionization may become important. In those conditions, thermodynamic properties depend on temperature and composition, and the energy equation must be solved with a more detailed gas model. The perfect-gas result remains useful as a baseline, but it should not be assumed to provide high-enthalpy accuracy without checking the temperature and composition range.

Implication: the present report uses this research as a theoretical baseline and does not claim to reproduce all the phenomena discussed in the wider literature.

2.22 High-temperature and hypersonic gas effects [14, 25, 26]

Hypersonic flows can produce very large temperature increases behind shocks, particularly near blunt bodies and in high-enthalpy facilities. Under these conditions, a calorically perfect gas may no longer represent the thermodynamic response of air. Variable specific heats, vibrational nonequilibrium, chemical dissociation and ionization can alter the relation between pressure, density, temperature and enthalpy. Anderson's high-temperature gas-dynamics text, cited in the source report, provides a broader framework for analysing these effects [14].

The main lesson for the present study is that the chosen $\gamma = 1.4$ model is an explicit assumption, not a universal property of air. The report's Mach-number range is treated using the same constant γ for consistency with the source calculations. For applications involving high post-shock enthalpy, the next step would be to replace the calorically perfect gas closure with temperature-dependent thermodynamic data or a thermochemical nonequilibrium model. Such extensions should be identified clearly because they change the governing property relations.

Relevance to this project: this topic establishes why a one-dimensional normal-shock calculation is a useful starting point, while also defining what it cannot predict.

2.23 Oblique shocks and their relation to normal shocks [1, 3, 18–23]

An oblique shock is inclined to the incoming flow rather than perpendicular to it. The upstream velocity can be decomposed into components normal and tangential to the shock. The normal component undergoes the compression associated with a normal shock, while the tangential component is unchanged for an inviscid shock in the absence of shear stress. Consequently, normal-shock relations can be applied to the normal Mach-number component to obtain the thermodynamic jump across an oblique shock.

This connection is important in supersonic inlets, where a sequence of oblique shocks is often used to compress and decelerate the flow before a terminal normal shock or subsonic diffuser. Compared with a single strong normal shock, a carefully designed sequence of weaker compression waves can reduce total-pressure loss. NACA Report 1135 includes both normal- and oblique-shock relations, allowing these configurations to be treated within one consistent framework [1]. The present report focuses on the normal-shock limiting case.

Critical observation: the analytical relations are strongest when the assumptions are stated explicitly and the upstream and downstream states are clearly defined.

2.24 Normal shocks in inlets, diffusers and nozzles [3, 14–17, 20–23]

In a supersonic inlet, the incoming air must be compressed and slowed before reaching a subsonic compressor. A terminal normal shock may convert the remaining supersonic flow to subsonic flow, but its stagnation-pressure loss reduces the pressure available to the engine. In a convergent-divergent nozzle, a normal shock may occur in the divergent section when the back pressure differs from the design condition. The resulting pressure rise and loss of total pressure alter the downstream flow and can affect thrust and separation.

The ideal normal-shock ratios provide a first estimate of the thermodynamic changes associated with such a shock. Component performance, however,

depends on the shock location, area variation, boundary-layer state, bleed, wall heat transfer and downstream operating condition. Therefore, the ratios should be combined with the rest of the inlet or nozzle analysis rather than used alone. The literature's emphasis on shock-boundary-layer interaction reflects the practical importance of these coupled effects [6], [9], [10].
Implication: the present report uses this research as a theoretical baseline and does not claim to reproduce all the phenomena discussed in the wider literature.

2.25 Detached bow shocks and blunt-body flows [14, 19, 20, 46–49]

When a supersonic stream encounters a blunt body, a detached bow shock forms ahead of the nose. Along the stagnation streamline, the shock is locally close to normal, so normal-shock theory is a useful first approximation for the immediate post-shock state. Away from the stagnation line, the shock is curved and the flow experiences oblique compression. The full field therefore requires a spatially varying treatment rather than one uniform normal-shock jump.
The temperature and pressure behind a strong bow shock are important in high-speed aerodynamics because they influence surface heating and the thermodynamic state of the gas approaching the body. At high enthalpy, real-gas effects can become significant, so the perfect-gas approximation may be insufficient. This application illustrates both the usefulness and the limits of the normal-shock model: it gives a clear local baseline, but detailed prediction requires shock curvature, viscous flow and high-temperature chemistry to be considered.
Relevance to this project: this topic establishes why a one-dimensional normal-shock calculation is a useful starting point, while also defining what it cannot predict.

2.26 Shock tubes, reflected shocks and test facilities [4, 20, 21, 46]

Shock tubes and shock tunnels are used to create short-duration high-speed test flows. The primary shock establishes a high-pressure, high-temperature region in the driven gas; after reflection, additional compression may occur. Experimental pressure histories can be influenced by boundary-layer growth, reflected-shock motion and facility geometry. Davies and Edwards' work on reflected-shock pressure-time profiles demonstrates the importance of comparing ideal wave theory with actual transient measurements [4].
For a steady normal-shock calculation, the shock-fixed frame provides a convenient way to relate the gas states. For an entire shock-tube experiment, however, the motion of the shock, contact surface and expansion fan must also be calculated. Thus, the jump equations are necessary but not sufficient for complete facility analysis. This separation between local jump conditions and global unsteady-wave behaviour is an important theme in experimental gas dynamics.
Critical observation: the analytical relations are strongest when the assumptions are stated explicitly and the upstream and downstream states are clearly defined.

2.27 Synthesis of literature and research gap [1–3, 10–13, 27–45]

The literature establishes the normal-shock jump relations as a mature and well-documented part of compressible-flow theory. NACA Report 1135 and NASA's educational equations provide accessible formulations, while gas-dynamics texts place the equations within the wider theory of compressible flow [1]–[3]. Experimental research on shock tubes and shock-boundary-layer interactions shows that real measurements may include transient, viscous and geometric effects that are absent from the ideal jump model [4]–[7]. Reviews of turbulence, three-dimensional interactions and control demonstrate the continuing importance of these more complex phenomena [8]–[13].
The specific gap addressed by the present project is not a lack of normal-shock theory. Rather, it is the need for a clearly organized and reproducible calculation that connects the classical equations to a consistent set of property ratios across a selected Mach-number range. The study therefore evaluates downstream Mach number, static pressure, density, temperature, total-pressure recovery and entropy change for air with $\gamma = 1.4$. It presents the results as a baseline and identifies the additional physics required for practical component prediction. This scope is appropriate for a focused analytical-numerical undergraduate investigation.
Implication: the present report uses this research as a theoretical baseline and does not claim to reproduce all the phenomena discussed in the wider literature.

3. PROBLEM STATEMENT AND OBJECTIVES

3.1 Problem Statement

The problem is to determine how the principal flow properties change when a supersonic stream of air passes through a stationary normal shock. The analysis uses a one-dimensional, adiabatic, calorically perfect-gas model and evaluates the standard normal-shock relations for upstream Mach numbers from 1.2 to 3.5.

3.2 Objectives

- To state the conservation equations governing a one-dimensional normal shock.
- To calculate downstream Mach number and static-property ratios for selected upstream Mach numbers.
- To quantify stagnation-pressure loss and entropy increase as shock strength changes.

• To demonstrate the dimensional meaning of the ratios using standard sea-level reference conditions.
• To present the results in clear tables and graphs suitable for preliminary aerodynamic analysis.

4. PHYSICAL MODEL AND THEORETICAL BACKGROUND

4.1 Physical Model

The shock is treated as stationary and normal to the incoming flow. State 1 denotes the uniform upstream condition and state 2 denotes the uniform downstream condition. The flow is steady and one-dimensional, with no heat transfer or shaft work. The gas is air represented by a constant ratio of specific heats, $\gamma = 1.4$. The finite internal shock structure is not resolved; its net effect is represented by the irreversible jump relations.

4.2 Assumptions

• Calorically perfect air with $\gamma = 1.4$.
• Steady, one-dimensional flow through the shock.
• Stationary shock surface perpendicular to the upstream flow.
• Adiabatic process with no shaft work.
• No chemical reactions, dissociation or ionization.
• Boundary-layer, turbulence and three-dimensional effects are excluded.

4.3 Physical Interpretation

Across a physically admissible normal shock, M1 > 1 and M2 < 1. Static pressure, density and temperature increase. Velocity decreases because mass flux is conserved while density increases. Total temperature remains constant in the adiabatic model, whereas total pressure decreases because entropy is generated.

5. GOVERNING EQUATIONS AND NUMERICAL METHOD

The jump relations are obtained by applying conservation laws to a control volume enclosing the shock. For a perfect gas, the equations reduce to the following working expressions.

Quantity	Relation
Conservation of mass	$\rho_1 V_1 = \rho_2 V_2$
Conservation of momentum	$p_1 + \rho_1 V_1^2 = p_2 + \rho_2 V_2^2$
Conservation of energy	$h_1 + V_1^2/2 = h_2 + V_2^2/2$
Downstream Mach number	$M_2^2 = [1 + (\gamma - 1)M_1^2/2] / [\gamma M_1^2 - (\gamma - 1)/2]$
Static pressure ratio	$p_2/p_1 = [2\gamma M_1^2 - (\gamma - 1)]/(\gamma + 1)$
Density ratio	$\rho_2/\rho_1 = [(\gamma + 1)M_1^2]/[(\gamma - 1)M_1^2 + 2]$
Static temperature ratio	$T_2/T_1 = (p_2/p_1)/(\rho_2/\rho_1)$
Velocity ratio	$V_2/V_1 = \rho_1/\rho_2$
Total temperature	$T_{o2}/T_{o1} = 1$ (adiabatic shock)
Total pressure ratio	$p_{o2}/p_{o1} = (p_2/p_1) \times [(1 + (\gamma-1)M_2^2/2)/(1 + (\gamma-1)M_1^2/2)]^{[\gamma/(\gamma-1)]}$
Entropy change	$\Delta s/R = [\gamma/(\gamma-1)] \ln(T_2/T_1) - \ln(p_2/p_1)$

5.1 Numerical Procedure

The upstream Mach number is specified and γ is fixed at 1.4. The downstream Mach number is evaluated first. The pressure and density ratios are then calculated, followed by the temperature ratio. The stagnation-pressure ratio and entropy change are evaluated from the corresponding perfect-gas relations. Calculations should retain adequate precision internally and round only for presentation. Static and stagnation properties must not be interchanged.

6. SAMPLE CALCULATION AND RESULTS

6.1 Sample Calculation for $M_1 = 2.0$

Given: $M_1 = 2.0$ and $\gamma = 1.4$.
$M_2 = \sqrt{\{[(1.4 - 1)(2.0)^2 + 2] / [2(1.4)(2.0)^2 - (1.4 - 1)]\}} = 0.5774$.
$p_2/p_1 = 1 + [2(1.4)/(1.4 + 1)](2.0^2 - 1) = 4.500$.
$\rho_2/\rho_1 = [(1.4 + 1)(2.0)^2] / [(1.4 - 1)(2.0)^2 + 2] = 2.6667$.

$T_2/T_1 = 4.500/2.6667 = 1.6875$.

6.1.1 Additional calculated properties

The sample is extended to include velocity, stagnation temperature, stagnation pressure and entropy change. For air, $R = 287$ J kg^{-1} K^{-1}, $\gamma = 1.4$, $T_1 = 288.15$ K and $a_1 = \sqrt{(\gamma RT_1)} \approx 340.3$ m/s. At $M_1 = 2.0$, $V_1 = M_1a_1 \approx 680.6$ m/s. The density ratio is 2.6667, so $V_2/V_1 = 1/2.6667 = 0.375$ and $V_2 \approx 255.2$ m/s. The downstream Mach number is 0.5774.

The downstream static temperature is $T_2 = 1.6875 \times 288.15 \approx 486.25$ K. The stagnation temperature is $T_0 = T(1 + 0.2M^2)$; upstream $T_{01} \approx 518.67$ K and downstream $T_{02} = 486.25[1 + 0.2(0.5774)^2] \approx 518.67$ K. The equality confirms conservation of total temperature for an adiabatic shock.

The stagnation-pressure recovery for $M_1 = 2.0$ is $p_{02}/p_{01} \approx 0.7209$. Thus, approximately 27.91% of the upstream stagnation pressure is lost across the shock. The entropy rise is $\Delta s = R \ln[(p_{01}/p_{02})] \approx 287 \ln(1/0.7209) \approx 93.7$ J kg^{-1} K^{-1}. This positive value is consistent with the irreversible nature of a shock.

6.1.2 Calculation sequence and checks

The calculation is checked in four ways: (i) M_2 must be less than unity for a normal shock with $M_1 > 1$; (ii) p_2, ρ_2 and T_2 must exceed their upstream values; (iii) T_{02}/T_{01} must equal unity for the stated adiabatic perfect-gas model; and (iv) p_{02}/p_{01} must be less than unity. A result violating any of these checks indicates a formula, unit or state-indexing error.

6.2 Dimensionless Results

M_1	M_2	p_2/p_1	ρ_2/ρ_1	T_2/T_1	p_{02}/p_{01}
1.2	0.8422	1.513	1.342	1.128	0.9928
1.5	0.7011	2.458	1.862	1.32	0.9298
1.8	0.6165	3.613	2.359	1.532	0.8127
2.0	0.5774	4.5	2.667	1.687	0.7209
2.5	0.513	7.125	3.333	2.137	0.499
3.0	0.4752	10.333	3.857	2.679	0.3283
3.5	0.451	14.125	4.261	3.315	0.2129

The values above retain the representative tabulated values from the source report. The trend is monotonic: as upstream Mach number increases, the downstream Mach number decreases and the static-property ratios rise, while stagnation-pressure recovery falls.

6.2.1 Interpretation of the tabulated values

The downstream Mach number falls continuously from 0.8422 at $M_1 = 1.2$ to 0.4510 at $M_1 = 3.5$. This confirms that the flow becomes subsonic immediately behind the normal shock and that stronger incident shocks produce greater deceleration. The static pressure ratio rises from 1.513 to 14.125, while the density ratio approaches the perfect-gas strong-shock limit $(\gamma + 1)/(\gamma - 1) = 6$ for $\gamma = 1.4$. The temperature ratio increases because the pressure rise is greater than the density rise.

6.2.2 Numerical consistency and physical bounds

For $\gamma = 1.4$, the strong-shock density ratio tends to 6 as M_1 becomes very large; the present maximum value, 4.261 at $M_1 = 3.5$, remains below this limit. The pressure ratio has no corresponding finite upper bound in the perfect-gas model. The total-pressure recovery decreases with Mach number, reflecting the increasing entropy production. These limits provide useful independent checks on the calculated table and graphs.

6.3 Dimensional Reference State

The source report uses $p_1 = 101.325$ kPa and $T_1 = 288.15$ K as standard sea-level reference conditions. The corresponding density is approximately 1.225 kg/m^3 and the upstream speed of sound is approximately 340.3 m/s. For $M_1 = 2.0$, the source reports $p_2 \approx 455.96$ kPa, $T_2 \approx 486.25$ K and $\rho_2 \approx 3.267$ kg/m^3.

6.4 Graphical Results

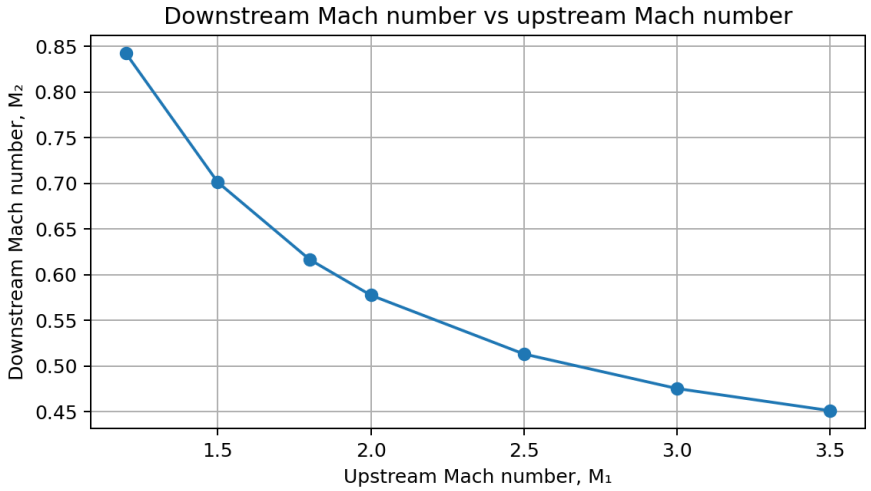


Figure 1. Downstream Mach number decreases as the upstream Mach number increases.

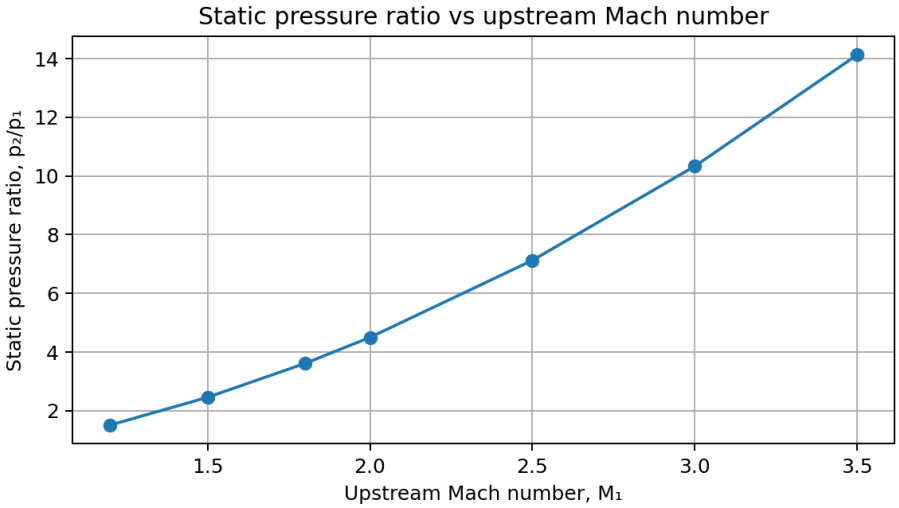


Figure 2. Static pressure ratio increases strongly with shock strength.

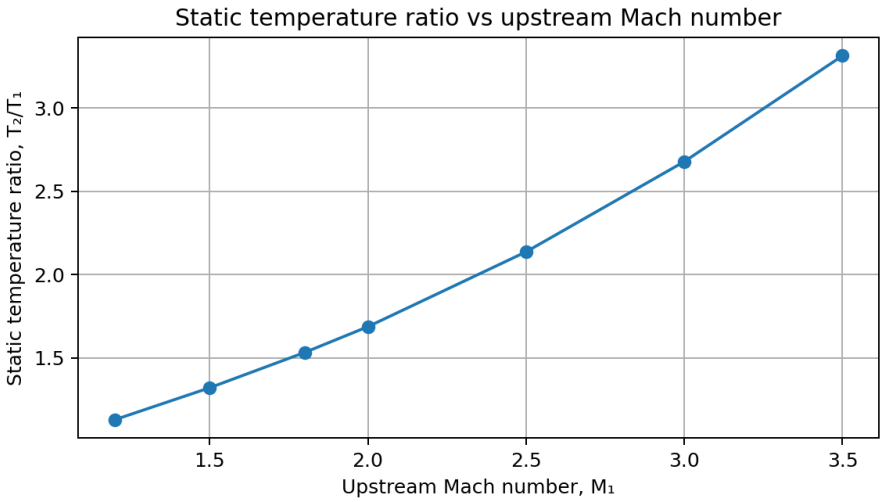


Figure 3. Static temperature ratio increases as kinetic energy is converted into internal energy.

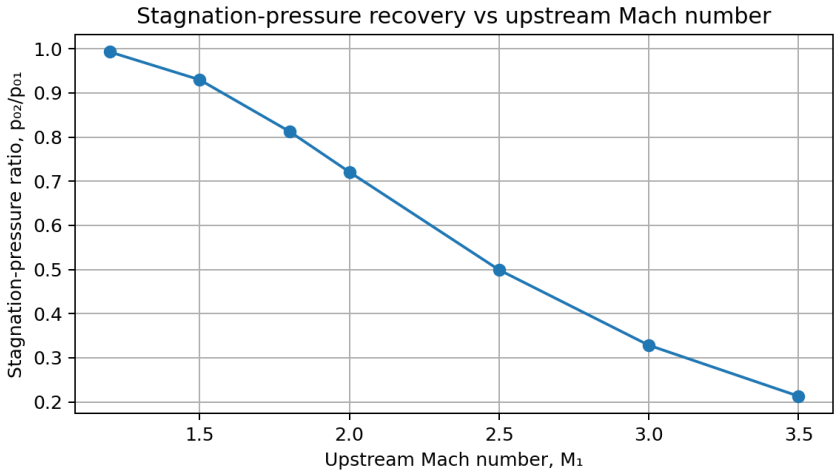


Figure 4. Stagnation-pressure recovery decreases as irreversibility increases.

7. DISCUSSION AND ENGINEERING APPLICATIONS

7.1 Discussion of Trends

The calculated results show that a normal shock converts a supersonic upstream stream into a subsonic downstream stream. Between $M_1 = 1.2$ and $M_1 = 3.5$, M_2 decreases from approximately 0.842 to 0.451. Over the same interval, p_2/p_1 increases from 1.513 to 14.125, ρ_2/ρ_1 increases from 1.342 to 4.261 and T_2/T_1 increases from 1.128 to 3.315. These changes demonstrate the increasing strength of the shock.

The stagnation-pressure ratio falls from 0.9928 to 0.2129 over the selected range. This is the principal performance penalty associated with a stronger normal shock. Entropy generation is positive for every supersonic case and increases with Mach number. The results are consistent with the second law and with the standard normal-shock framework.

7.2 Engineering Applications

Supersonic inlets

A terminal normal shock can decelerate supersonic inlet flow to subsonic conditions. Its pressure rise is accompanied by stagnation-pressure loss, which affects the pressure delivered to downstream engine components.

Nozzles and diffusers

A normal shock may occur in a convergent-divergent nozzle when the operating back pressure differs from the design condition. The shock changes the downstream state and can influence nozzle performance.

Shock tubes

Shock-tube analysis uses shock-fixed jump relations to estimate the state behind a moving shock. Additional unsteady-wave relations are needed for the complete facility.

Blunt-body aerodynamics

The stagnation-line portion of a detached bow shock is locally close to normal, making normal-shock theory a useful first estimate of the post-shock state.

8. LIMITATIONS AND FUTURE SCOPE

8.1 Limitations

- The gas is assumed to be calorically perfect with constant $\gamma = 1.4$.
- The flow is treated as steady and one-dimensional.
- Boundary-layer interaction, shock-induced separation, turbulence and three-dimensional effects are not included.
- High-temperature real-gas effects such as variable specific heat, dissociation and ionization are neglected.
- The study is analytical-numerical and is not a substitute for experimental or high-fidelity CFD validation.

8.2 Future Scope

Future work can extend the analysis to oblique shocks, Prandtl–Meyer expansion waves and complete convergent-divergent nozzle systems. The

analytical results can be compared with a CFD solution or wind-tunnel measurements. Further extensions may include variable specific heats, real-gas thermochemistry, boundary-layer interaction, shock-induced separation and three-dimensional inlet geometries. These additions should be introduced as separate modelling stages so that the influence of each new physical effect can be assessed.

9. CONCLUSION

A numerical investigation of normal-shock behaviour in supersonic air has been presented using the standard one-dimensional perfect-gas relations. The equations are based on conservation of mass, momentum and energy, together with the ideal-gas model and $\gamma = 1.4$. The results show that the downstream Mach number remains subsonic and decreases as the upstream Mach number increases. Static pressure, density and temperature rise across the shock, while stagnation pressure decreases because entropy is generated.

For the investigated range, $M_1 = 1.2$ to 3.5, the pressure ratio increases from approximately 1.513 to 14.125, the density ratio from 1.342 to 4.261 and the temperature ratio from 1.128 to 3.315. Stagnation-pressure recovery decreases from 0.9928 to 0.2129. These trends confirm that stronger normal shocks produce larger static-property changes and more severe irreversible losses. The expanded literature survey shows that this ideal solution is a fundamental reference, while experiments and practical aerospace flows require additional consideration of viscous, turbulent, unsteady, three-dimensional and high-temperature effects.

REFERENCES

[1] Ames Research Staff, “Equations, Tables, and Charts for Compressible Flow,” NACA Report 1135, 1953. NASA Technical Reports Server: https://ntrs.nasa.gov/citations/19930091059.

[2] NASA Glenn Research Center, “Normal Shock Wave Equations,” Beginner’s Guide to Aeronautics. https://www.grc.nasa.gov/www/k-12/airplane/normal.html.

[3] J. D. Anderson, Jr., Modern Compressible Flow: With Historical Perspective, 3rd ed., McGraw-Hill, 2003.

[4] L. Davies and D. H. Edwards, “An experimental investigation of the reflected-shock pressure-time profiles for air, oxygen, nitrogen, argon, carbon dioxide and acetylene,” Journal of Fluid Mechanics, 1964.

[5] C. duP. Donaldson, “Effects of Interaction Between Normal Shock and Boundary Layer,” NACA, 1944.

[6] J. E. Green, “Interactions between shock waves and turbulent boundary layers,” Progress in Aerospace Sciences, vol. 11, pp. 235–340, 1970.

[7] G. G. Mateer, A. Brosh, and J. R. Viegas, “A normal shock-wave turbulent boundary-layer interaction at transonic speeds,” AIAA Paper 76-161, 1976.

[8] Y. Andreopoulos, J. H. Agui, and G. Briassulis, “Shock wave–turbulence interactions,” Annual Review of Fluid Mechanics, vol. 32, pp. 309–345, 2000.

[9] J. Delery, J. G. Marvin, and E. Reshotko, Shock-Wave Boundary-Layer Interactions, AGARDograph 280, NATO, 1986.

[10] P. M. Ligrani, E. S. McNabb, H. Collopy, M. Anderson, and S. M. Marko, “Recent investigations of shock wave effects and interactions,” Advances in Aerodynamics, vol. 2, article 4, 2020. https://doi.org/10.1186/s42774-020-0028-1.

[11] D. V. Gaitonde and M. C. Adler, “Dynamics of three-dimensional shock-wave/boundary-layer interactions,” Annual Review of Fluid Mechanics, vol. 55, pp. 291–321, 2023. https://doi.org/10.1146/annurev-fluid-120720-022542.

[12] K. Sabnis and H. Babinsky, “A review of three-dimensional shock wave–boundary-layer interactions,” Progress in Aerospace Sciences, 2023.

[13] T. Jana and M. Kaushik, “Survey of control techniques to alleviate repercussions of shock-wave and boundary-layer interactions,” Advances in Aerodynamics, vol. 4, article 27, 2022.

[14] J. D. Anderson, Jr., Hypersonic and High-Temperature Gas Dynamics, 2nd ed., AIAA, 2006.

[15] S. M. Yahya, Fundamentals of Compressible Flow with Aircraft and Rocket Propulsion, 4th ed., New Age International, 2011.

[16] E. Rathakrishnan, Gas Dynamics, 2nd ed., Prentice Hall of India, 2010.

[17] E. Rathakrishnan, Applied Gas Dynamics, Wiley, 2010.

[18] NASA Glenn Research Center, “Oblique Shock Waves,” Beginner’s Guide to Aeronautics. https://www.grc.nasa.gov/www/k-12/airplane/oblique.html.

[19] R. Courant and K. O. Friedrichs, Supersonic Flow and Shock Waves, Interscience, 1948.

[20] H. W. Liepmann and A. Roshko, Elements of Gasdynamics, Wiley, 1957.

[21] A. H. Shapiro, The Dynamics and Thermodynamics of Compressible Fluid Flow, Vols. I–II, Ronald Press, 1953.

[22] M. J. Zucrow and J. D. Hoffman, Gas Dynamics, Vol. I, Wiley, 1976.

[23] P. A. Thompson, Compressible-Fluid Dynamics, McGraw-Hill, 1972.

[24] W. H. J. Sutton and A. G. S. Sutton, Rocket Propulsion Elements, 9th ed., Wiley, 2017.

[25] R. W. Zucker and O. Biblarz, Fundamentals of Gas Dynamics, 2nd ed., Wiley, 2002.

[26] J. F. Clarke and M. McChesney, The Dynamics of Real Gases, Butterworths, 1964.

[27] J. D. Anderson, Computational Fluid Dynamics: The Basics with Applications, McGraw-Hill, 1995.

[28] C. Hirsch, Numerical Computation of Internal and External Flows, Vol. 2, Wiley, 1990.

[29] R. J. LeVeque, Finite Volume Methods for Hyperbolic Problems, Cambridge University Press, 2002.

[30] E. F. Toro, Riemann Solvers and Numerical Methods for Fluid Dynamics, 3rd ed., Springer, 2009.

[31] P. L. Roe, "Approximate Riemann solvers, parameter vectors, and difference schemes," Journal of Computational Physics, vol. 43, pp. 357–372, 1981.

[32] B. van Leer, "Towards the ultimate conservative difference scheme. V. A second-order sequel to Godunov's method," Journal of Computational Physics, vol. 32, pp. 101–136, 1979.

[33] A. Harten, "High resolution schemes for hyperbolic conservation laws," Journal of Computational Physics, vol. 49, pp. 357–393, 1983.

[34] P. L. Roe, "Characteristic-based schemes for the Euler equations," Annual Review of Fluid Mechanics, vol. 18, pp. 337–365, 1986.

[35] J. L. Steger and R. F. Warming, "Flux vector splitting of the inviscid gasdynamic equations with application to finite-difference methods," Journal of Computational Physics, vol. 40, pp. 263–293, 1981.

[36] A. Jameson, W. Schmidt, and E. Turkel, "Numerical solution of the Euler equations by finite volume methods using Runge-Kutta time-stepping schemes," AIAA Paper 81-1259, 1981.

[37] S. K. Godunov, "A difference method for numerical calculation of discontinuous solutions of the equations of hydrodynamics," Matematicheskii Sbornik, vol. 47, pp. 271–306, 1959 (English translation).

[38] P. D. Lax, "Weak solutions of nonlinear hyperbolic equations and their numerical computation," Communications on Pure and Applied Mathematics, vol. 7, pp. 159–193, 1954.

[39] R. D. Richtmyer and K. W. Morton, Difference Methods for Initial-Value Problems, 2nd ed., Interscience, 1967.

[40] P. Colella and P. R. Woodward, "The piecewise parabolic method (PPM) for gas-dynamical simulations," Journal of Computational Physics, vol. 54, pp. 174–201, 1984.

[41] P. Woodward and P. Colella, "The numerical simulation of two-dimensional fluid flow with strong shocks," Journal of Computational Physics, vol. 54, pp. 115–173, 1984.

[42] G. A. Sod, "A survey of several finite difference methods for systems of nonlinear hyperbolic conservation laws," Journal of Computational Physics, vol. 27, pp. 1–31, 1978.

[43] D. S. Balsara, "Divergence-free adaptive mesh refinement for magnetohydrodynamics," Journal of Computational Physics, vol. 174, pp. 614–648, 2001.

[44] D. S. K. Yee, "A class of high-resolution explicit and implicit shock-capturing methods," NASA TM-89464, 1987.

[45] D. Knight, H. Yan, A. G. Panaras, and A. Zheltovodov, "Advances in CFD prediction of shock wave turbulent boundary layer interactions," Progress in Aerospace Sciences, vol. 39, pp. 121–184, 2003. https://doi.org/10.1016/S0376-0421(02)00069-6.

[46] D. Ranjan, J. Oakley, and R. Bonazza, "Shock-bubble interactions," Annual Review of Fluid Mechanics, vol. 43, pp. 117–140, 2011. https://doi.org/10.1146/annurev-fluid-122109-160744.

[47] G. Ben-Dor, Shock Wave Reflection Phenomena, 2nd ed., Springer, 2007.

[48] G. Ben-Dor, Shock Wave Reflection Phenomena, Springer, 1992.

[49] J. D. Anderson, "A history of aerodynamics and its impact on high-speed flight," Cambridge University Press, 1997.

[50] R. J. Goldstein (ed.), Fluid Mechanics Measurements, 2nd ed., Taylor & Francis, 1996.